Scientific Research Publishing

International Journal of Geosciences, 2023, 14, 619-634
https://www.scirp.org/journal/ijg
ISSN Online: 2156-8367
ISSN Print: 2156-8359

Research on Deformation Mode of the Longmenshan-Longriba Region Using GPS and Leveling Data

Xudong Li[1], Wei Li[1,2*], Jiangtao Qiu[1], Bing Feng[1], Xiang Liu[1]

[1]The Second Monitoring and Application Center, China Earthquake Administration, Xi'an, China
[2]Institute of Geology, China Earthquake Administration, Beijing, China
Email: *15727399488@163.com

How to cite this paper: Li, X.D., Li, W., Qiu, J.T., Feng, B. and Liu, X. (2023) Research on Deformation Mode of the Longmenshan-Longriba Region Using GPS and Leveling Data. *International Journal of Geosciences*, **14**, 619-634.
https://doi.org/10.4236/ijg.2023.147033

Received: June 3, 2023
Accepted: July 23, 2023
Published: July 26, 2023

Abstract

The Longmenshan-Longriba region is located on the eastern edge of the Tibetan Plateau, and is an ideal place to study the eastward extrusion and uplift mechanism of the plateau. Previous studies on this area mainly focused on tectonic activity and seismic hazard, with few studies giving its overall deformation characteristics and dynamic mechanism. This paper uses the latest dense GPS data, combined with precise Leveling data to analyze the kinematic characteristics and deformation mode of the Longmenshan fault zone (LMSF) and the Longriba fault zone (LRBF). The results show that both the Longmenshan fault zone and the Longriba fault zone have certain right-lateral strike-slip and thrusting, indicating that they play an important role in adjusting strain distribution and absorbing tectonic deformation; The strain-rate field on the Longriba fault zone is broadly distributed, suggesting that the deformation field is at least partially coupled; while the strain-rate field on the Longmenshan fault zone presents a non-uniform distribution, indicating different dynamic sources acting on segments. The high strain rate areas revealed in this study points us to the high-risk area for future earthquakes. The present-day vertical motion velocity field in the region obtained from Leveling and GPS data shows a mismatch between the regional deformation field and active tectonics, which can be explained by the incomplete coupling of deformation between the lower and upper crust.

Keywords

Longmenshan Fault Zone, Longriba Fault Zone, GPS, Strain, Leveling

1. Introduction

With the collision of the Indian and Eurasian plates since the Cenozoic, the Ti-

betan Plateau continued to be extruded eastward, and the Longmenshan fold-thrust belt with steepest topography gradient was formed on the eastern margin. The lower crustal flow model has explained the high topographic gradient, low shortening, and missing foreland deposits of the Longmen Shan [1]. This model emphasizes non-tectonic uplift within blocks, without tectonic deformation on boundary faults. The M8.0 Wenchuan earthquake in 2008 was a typical thrust fault type earthquake, which raising the upper crustal brittle deformation to the uplift mechanism and deformation pattern of the region. Through seismic reflection profiles, the restored strata from the Longmen Shan to the Sichuan basin, proves a matching relationship between the tectonic shortening and topography of the eastern margin of the Tibetan Plateau, and thus leading to the upper crustal brittle shortening model [2].

In 2013, the M7.0 Lushan earthquake occurred in the southern Longmen Shan. The epicenter of this earthquake was located in the foreland of the southern Longmen Shan where the Coulomb stress increased due to the Wenchuan earthquake. It was a typical blind thrust earthquake [3]. The biggest feature of the southern segment of Longmen Shan compared with the central and northern segments is that the faults are scattered and extend to the interior of the Sichuan basin. Many fault-related folds developed in the foreland and the internal basin, such as the Mengdingshan anticline, the Xiongpo anticline, and the Longquanshan anticline. The deformation pattern and strain distribution of the southern Longmen Shan are far more complex than those of the central and northern Longmen Shan [4].

The Longriba fault zone (LRBF) is a secondary block boundary inside the Bayan Har block. Deep seismic reflection profiles across it revealed that the fault staggered the Moho surface below the plateau [5]. Additionally, the fault is also a geomorphological boundary, with a very flat plateau to the west, and the highly undulating Longmen Shan to the east. The southwestern and northeastern segments of the fault might have also been active since the late Quaternary [6], while field investigation shows that the late Pleistocene alluvial terraces have not been faulted. Along the middle segment of the LRBF, linear tectonic and geomorphological features are well-developed, indicating that it has intensive activity since the late Quaternary. The LRBF is dominated by dextral strike-slip with a southeastward thrust component, which has the capacity to generate earthquakes of magnitude >7. The slip rate of the LRBF decreased from ~7.5 mm/yr in the late Pleistocene to ~2.1 mm/yr in the Holocene, which may be related to the weakening of the eastward movement of the Tibetan Plateau [7]. Compared with the Longmenshan fault zone, the LRBF plays an important role in the strain distribution of the eastern margin of the plateau [7].

According to the latest GPS observation, a shortening rate of about 5 mm/yr exists in the range of about 400 km between the Songpan-Ganzi area and the Longmenshan fault zone [8]. This scattered deformation must be due to the existence of multiple faults [8]. In addition, there is a dextral strike-slip of about 1 mm/yr across the Longmenshan fault zone, while the dextral strike-slip can

reach up to 8 mm/yr in the Songpan-Ganzi area, mainly distributed on both sides of the LRBF, indicating that the Longriba fault zone may have a high dextral slip and a wider strain zone.

From the locations and rupture scales of the Wenchuan earthquake and Lushan earthquake, it can be inferred that the Longmenshan fault zone has so mature segmentation that different segments have different seismogenic structures, which could generate large earthquakes alone. Although weak seismic activity in the LRBF nowadays, high slip rate, segmentation and mature structures reminds us the seismic risk cannot be ignored. Therefore, this paper attempts to use the latest GPS data, combined with Leveling data to analyze the present deformation pattern and kinematic characteristics of the region, explaining its future seismic hazard and dynamic mechanism. Our work can provide new slip rates for the kinematics of the LMSF-LRBF and a basis for seismic risk assessment. A three-dimensional kinematic field of the study area provides new constraints on the mechanisms deforming the eastern Tibet and to illuminate the spatial arrangement of the processes involved. The kinematic field supports us to detect and distinguish the localized deformation by fault creep in the upper crust and mid-crust as well as distributed deformation in the lower crust and upper mantle.

2. Regional Seismotectonic Setting

The Longmenshan fault zone (LMSF) is NE-trending along the eastern margin of the Tibetan Plateau, with a total length of 580 km, forming the boundary between the Bayan Har block and the Sichuan basin [9]. It is generally composed of three major faults, the Wenchuan-Maoxian fault (WMF), the Beichuan-Yingxiu fault (BYF) and the Jiangyou-Guanxian fault (JGF), which can be roughly divided into three segments. The middle and northern segments are about 40 - 50 km wide, and no foreland fold-belt developed; the southern segment is about 80 km wide, consisting of six branch faults and a foreland fold-belt of ~90 km (**Figure 1**, [4]). The 2008 Wenchuan M8.0 earthquake ruptured simultaneously the BYF and the JGF, forming a 240 km long surface rupture zone and a fault scarp up to 8.6 m [10] [11].

Geology and geodesy show that the total vertical thrusting or shortening rate across the LMSF is probably no more than 3 mm/yr, and the strike-slip and thrust rate on single fault is probably no more than 1 mm/yr [12] [13] [14] [15].

The Longriba fault zone (LRBF) is located about 200 km northwest of the LMSF, roughly parallel to LMSF, dividing the Bayan Har block into the Aba sub-block and the Longmenshan sub-block. The Aba sub-block is characterized by a series of NW-trending left-lateral strike-slip faults, accompanied by the eastward movement of the Bayan Har block; while the Longmenshan sub-block is characterized by strong tectonic shortening and orogeny, accompanied by NE-SW-oriented large thrust faults and fault-related folds. The LRBF was first described as a dextral shear zone by GPS measurements [16]. The LRBF is dominated by dextral slip with a southeastward thrust component, and considered to be a newly formed fault in the late Quaternary [6].

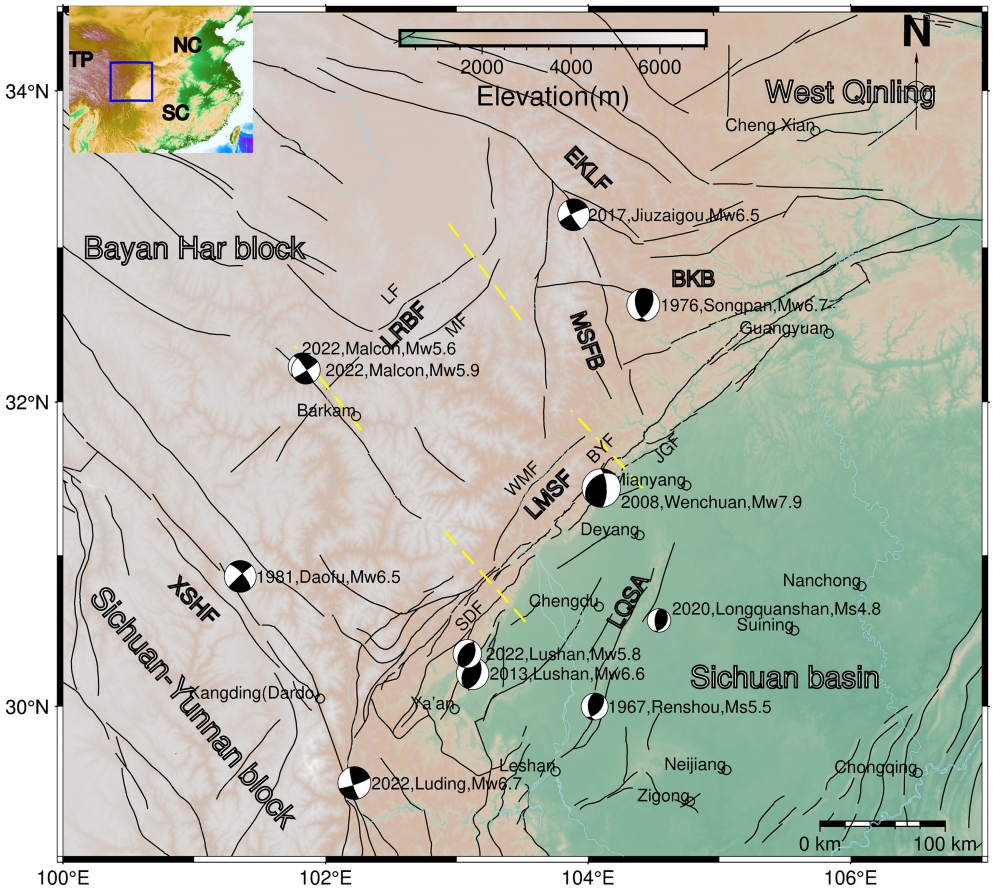

Figure 1. Sketch map of seismo-tectonic background in the study area. Epicenters and focal mechanisms after 1970 from Global Centroid-Moment Tensor seismic catalog (see Data and Resources). Black solid line represents active faults. Yellow dotted lines indicate fault segments. Blue solid line represents rivers. LRBF = Longriba Fault zone; LMSF = Longmenshan Fault zone; EKLF = Eastern Kunlun Fault; MSFB = Minshan faulted block; LQSA = Longquanshan Anticline; XSHF = Xianshuihe Fault zone. JGF = Jiangyou-Guanxian fault; BYF = Beichuan-Yingxiu fault; WMF = Wenchuan-Maoxian fault; SDF = Shuangshi-Dachuan fault; LF = Longriqu fault; MF = Maoergai fault; The inset map shows the location of the the study area. TP = Tibetan Plateau; NC = North China; SC = South China.

The LRBF consists of two branch faults, namely the Longriqu fault (LF) on the northwest side and the Maoergai fault (MF) on the southeast side. These two branch faults are nearly parallel and separated by about 20 - 30 km (**Figure 1**). This type is somewhat similar to the surface ruptures of the Wenchuan earthquake [7]. The paleoearthquake history of the LF is recovered by excavating trenches, combined with field surveys and chronological data. The latest four rupture events on the LF occurred at 5080 ± 90, 11,100 ± 380, 13,000 ± 260, and 17,830 ± 530 cal yr B.P., respectively, and the last event probably ruptured both the LF and MF [7]. Through remote sensing interpretation combined with field investigations, the southeastern branch of the southern LRBF is found to have late Quaternary activities, and is dominated by dextral slip with thrust component. The activity intensity of the southern segment of the LRBF is weaker than that of the middle segment [17].

3. Methods and Results

3.1. GPS Velocity Field

The principal data used for this study come from multiple sources and was published by Wang [8], in which the procedures of data collection and processing are described in detail. We select 256 GPS regional stations with a large number of observation periods in the South China block, and calculate the Euler pole parameters of the South China block under the Eurasian framework. After deduction, the GPS velocity field relative to the South China block was obtained (**Figure 2(a)**).

A method for interpolation of sparse two-dimensional vector data, based on the Green's functions of an elastic body subjected to in-plane forces, is used to detect the movement of the crustal blocks [18]. Although GPS sites in the region are sparse (**Figure 2(a)**), the typical spacing of GPS points ranging from 50 to 150 km, the method is also useful to measure strain localization as well as strain accumulation. We have adopted a new module "gpsgridder" built into the Generic Mapping Tools (GMT) [19] to achieve a interpolated 2-D velocity field derived from original geodetic measurements (**Figure 2(b)**). The grid spacing is set to 20 × 20 arc minute for reliability and reasonableness.

The interpolated 2-D velocity field shows a clear motion trend map with high consistency to the original GPS motion vectors (**Figure 2(b)**). The interior of the Bayan Har block moves coherently in the NEE direction. The direction and magnitude of the motion vector change significantly on both sides of the LRBF. The magnitude of the motion vector on both sides of the LMSF does not change significantly, while manifested as a change in direction. The Sichuan-Yunnan block moves SE at a faster rate, accompanied by clockwise rotation of the vectors.

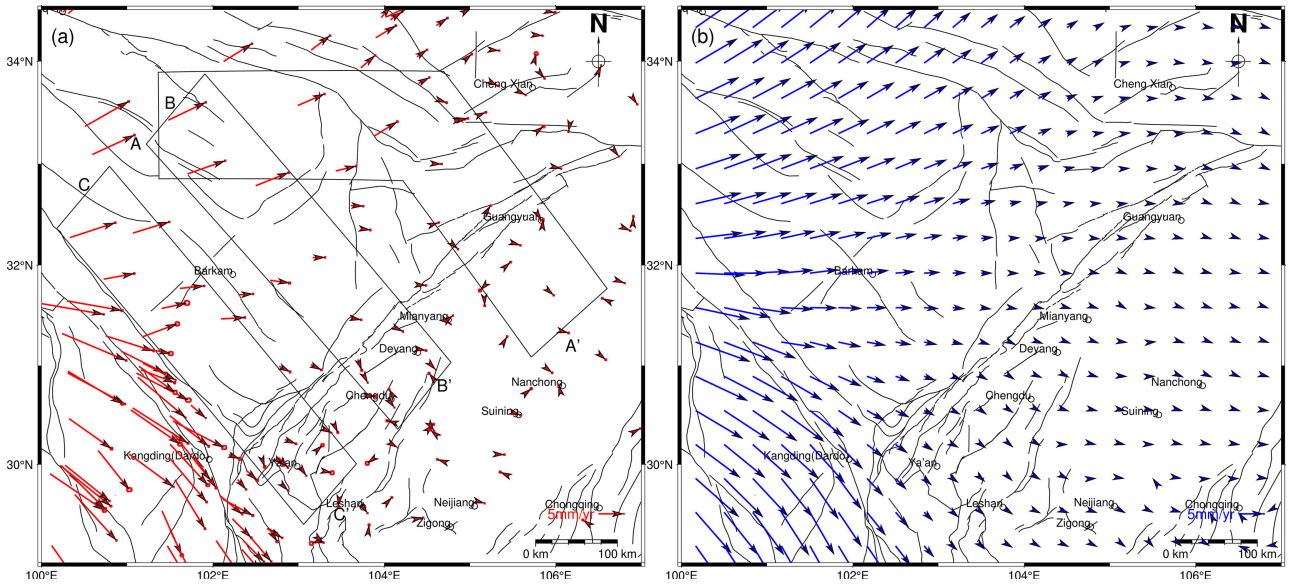

Figure 2. (a) GPS velocity field relative to the South China block, the GPS data are from Wang [8], and the black rectangles denotes GPS profiles in **Figure 3**. Black solid line represents active faults. (b) Interpolated GPS velocity field relative to the South China block produced by the method of Sandwell [18], the GPS data are from Wang [8]. Black solid line represents active faults.

Three velocity profiles were extracted perpendicular to the LMSF and LRBF, and the velocity vectors were projected in the direction of normal and parallel to faults, respectively (**Figure 2(a)**, **Figure 3**). The velocity profiles across the northern segment of the LMSF-LRBF shows both right-lateral strike-slip and thrust component on the northern segment of the LMSF close to ~1.3 mm/yr (**Figure 3(a)** and **Figure 3(b)**), which is consistent with the geological rates and lower seismicity with respect to the central and southern segment [20] [21]; while the dextral strike-slip and thrust component of the northern segment of the LRBF are 1.2 mm/yr and ~4.5 mm/yr, respectively, indicating that the LRBF as the northeastern border of the Bayan Har block functioned to accumulating crustal strain, and absorbing and adjusting tectonic deformation.

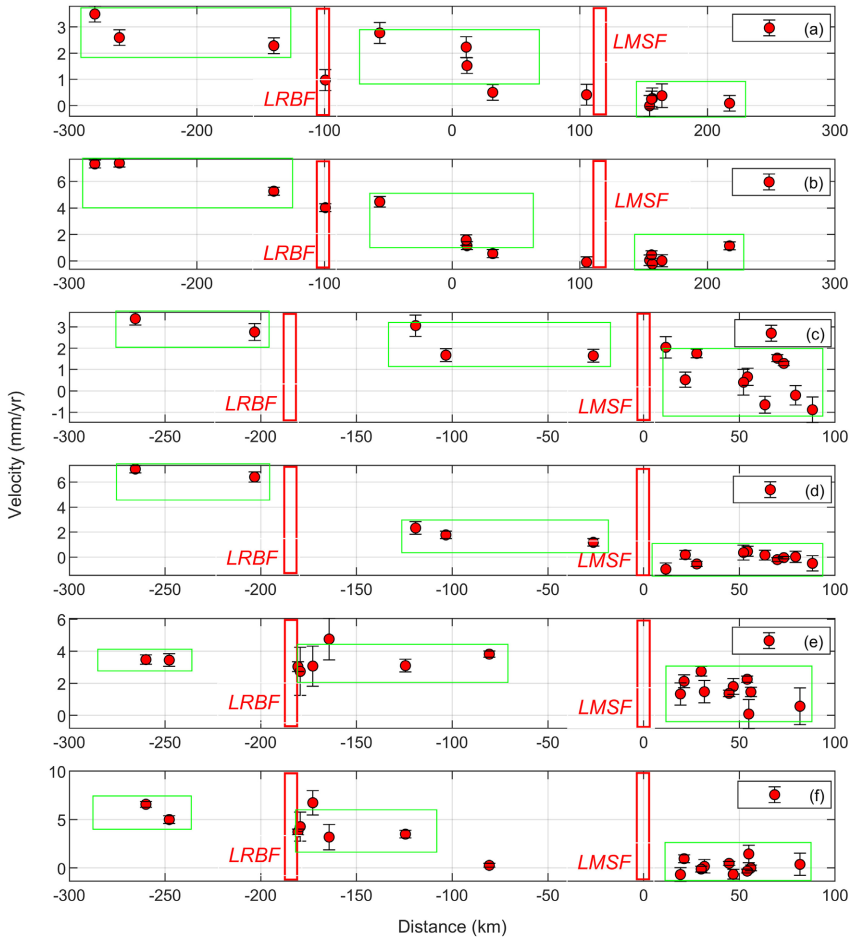

Figure 3. GPS profiles. The abscissa represents the distance, and the ordinate represents the velocity, applicable to each panel. (a) and (b) represent the velocity components (mm/yr) of the normal and parallel to faults, respectively, corresponding to the A-A' in **Figure 2**; (c) and (d) represent the velocity components (mm/yr) of the normal and parallel to faults, respectively, corresponding to the BB' in **Figure 2**; (e) and (f) represent the velocity components (mm/yr) of the normal and parallel to faults, respectively, corresponding to the C-C' in **Figure 2**; LRBF: Longriba fault zone; LMSF: Longmenshan fault zone; Red rectangles represent fault locations. Green rectangles represent acceptable ranges of the velocities. We estimate the slip rates of faults by calculating the differences in the average site velocities on both sides of the faults.

According to **Figure 3(c)** and **Figure 3(d)**, the velocity profiles across the middle segment of the LMSF-LRBF gives that although the middle segment of the LMSF has a ~1.9 mm/yr right-lateral slip with ~1.3 mm/yr thrust component, they do not exceed ~3 mm/yr, which is consistent with previous GPS and geological researches [12] [14] [15] [22]; The thrust component across the middle segment of the LRBF equals to ~1 mm/yr, while the dextral slip can reach 4 - 5 mm/yr, indicating that the middle segment of the LRBF is mainly dominated by shear deformation. The high dextral slip rate is conducive to the uniform distribution of stress and strain on the entire fault zone, and weakens the locking effect caused by the continuous extrusion of the block [23].

The dextral slip and thrust component across the southern segment of the LMSF have similar characteristics to that of the middle segment, and ranging in ~1 - 2 mm/yr, which is consistent with geological researches in southern Longmen Shan (**Figure 3(e)** and **Figure 3(f)**, [4] [24]); Thrust and dextral slip in the southern segment of the LRBF also have similar characteristics to that of its middle segment, what different is that the slip rate is lesser, which is <1 mm/yr and approximates 3 mm/yr, respectively. Our GPS results reveal that the activity on the southwestern LRBF is mainly manifested by strike-slip movement and weak thrusting, which is in accordance with He [17]. There are few studies on the southern segment of the LRBF, and it is generally believed that its activity is weak or inactive. The above researches prove that the southern segment of the LRBF, together with its middle segment as a whole and continuous tectonic zone, may play an equally important role in the process of absorbing and distributing the stress and strain on the block boundary. The future seismic risk of the region should be revisited.

3.2. Strain Rate Field

A distance-weighted, least squares approach, developed by Shen [25], provides an improved approach to get strain rate map without using a priori information about fault locations and orientations. We calculate the strain rate field in the Longmenshan-Longriba region with a grid of $0.1^\circ \times 0.1^\circ$ (**Figure 4**).

Strain rate map depicted that the area with the highest strain is the Xianshuihe fault zone and its vicinity, consistent with its high sinistral slip rate and frequent seismicity (**Figure 1**, **Figure 4**, [26] [27]); The second area is the Longriba fault zone and the Minshan faulted block, extending towards NE to the easternmost edge of the Eastern Kunlun fault. The strain zone exhibits a relatively continuous and uniform distribution along the northeast-southwest trend, and strongly related to the strike and range of the LRBF. The strain field in the southern segment of the LRBF may have been affected by slip and locking of the Xianshuihe fault at the boundary of the Sichuan-Yunnan block (**Figure 4**). The strain rate in the Sichuan basin is the weakest, which is due to the stable craton basement and complete crustal structure. Only in the foreland of the southern Longmen Shan, local strain grows at the Longquanshan anticline. The Longquanshan fault zone

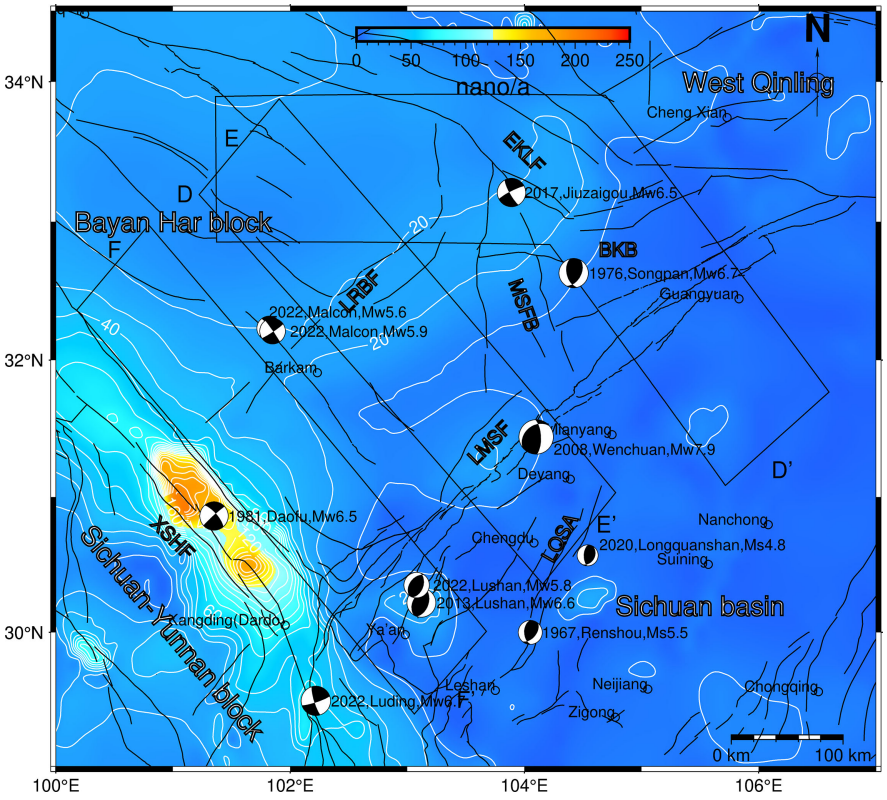

Figure 4. Strain rate map in the Longmenshan-Longriba region from GPS data. (unit: 1 nano/a = 1 × 10^{-9}/a). The solid white line is the contour. The black rectangles denote strain rate profiles in **Figure 5**. Other content is the same as **Figure 1**.

has high tectonic activity since the late Quaternary. Some moderate earthquakes have occurred near the Longquanshan anticline in recent years (**Figure 1**, **Figure 4**, [24] [28] [29]).

Unlike the LRBF, the LMSF does not show an distributed strain field along the fault, but it is noteworthy that two high-strain zones lies in the middle segment of the LMSF and the foreland of the southern LMSF, corresponding to the epicenters of the 2008 Wenchuan earthquake and the 2013 Lushan earthquake (**Figure 4**). After these two major earthquakes, the strain in these two areas perhaps has weakened, but it does not affect our findings that why the two large earthquakes happened in these two areas! Based on our strain field, combined with the regional active tectonics, it can be inferred that these two areas will still be locations of accumulation of strain and high-risk areas for major earthquakes in the future.

Low-temperature thermochronology on the southern segment of the LMSF pointed out that there are obvious differences in tectonic activity between the southern and middle segments of the LMSF. The activities of the middle segment are concentrated in the BYF and the JGF. The activities of the southern segment are scattered on the wider Shuangshi-Dachuan fault as well as the faults and folds of its footwall [30]. The tectonic deformation by million-year-scale low-temperature thermochronology is consistent with tectonic activity revealed

by the GPS-derived strain field (Figure 4).

In order to understand the variation of the strain rate on both sides of the fault and their relationship, three strain rate profiles were extracted, and the positions of them were the same as those of the velocity field profiles (Figure 4(a), Figure 5).

The D-D' profile in Figure 5 shows that the strain rate across the northern segment of the LMSF has an obvious increase, reaching 20 nano/yr, while the growth trend of the strain rate across the northern segment of the LRBF is weak, which may be due to the influence of the activity and shielding of the Minshan faulted block, resulting in high strain area mainly concentrated in the interior of the Minshan faulted block; From E-E' profile, we note that the strain rates of the middle segments of the LMSF and the LRBF have similar characteristics of rapid increase, and the maximum magnitude of strain rate is basically the same ~20 nano/yr. The only difference is that the strain distribution on both sides of the LRBF is wide ~150 km, while the other is within a narrow range ~50 km. The cause of the Wenchuan earthquake could be the rapid rise in local strain; F-F' profile, across the southern segment of the LMSF-LRBF, tells that the strain rate does not change significantly as observed in E-E' profile, but its magnitude is ~2 - 3 times that of the middle segment, and generally shows the tendency of increasing from SE to NW, which might be affected by the strike-slip movement of the Xianshuihe fault zone.

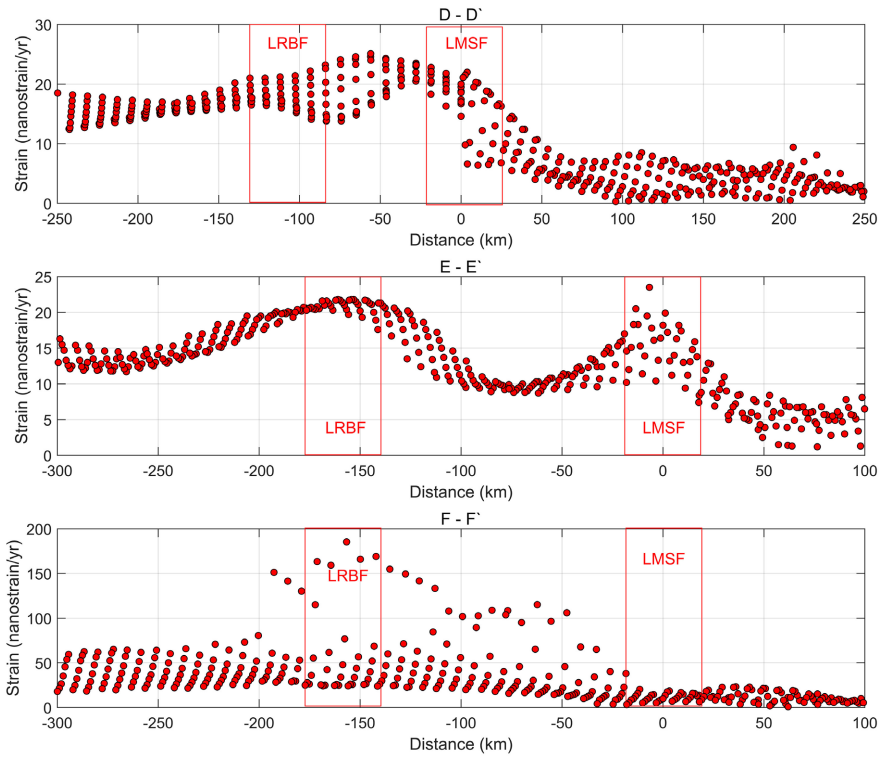

Figure 5. Strain rate profiles. The position of the profile can be found in Figure 4. The red rectangles represent the approximate range of the faults. LRBF = Longriba Fault zone; LMSF = Longmenshan Fault zone.

3.3. Vertical Velocity Field

In order to obtain the long-term interseismic deformation, we used two different sets of data to present the vertical velocity field in the Longmenshan-Longriba region (**Figure 6(a)**. One is from high-precision Leveling data measured between 1970 and 2012, which is processed and published by Hao [31]. The other one comes from a high-resolution GPS-derived 3-D velocity field for the present-day crustal movement of the Tibetan Plateau [32]. We compiled these two sets of data together and then put the coordinate system into the framework of ITRF2008.

The reverse dip-slip rates along the Longmen Shan and Longriba fault systems are 4.2 ± 0.5 and 2.8 ± 0.3 mm/a respectively with the locking depth of 22 km [31]. However, the Leveling profile displays that the vertical deformation on both sides of the LMSF and LRBF was not completely controlled by the faults (**Figure 6(a)**, therefore we infer distributed deformation on both sides of the faults and decoupling between surface deformation and deep driving.

To better describe the regional deformation and illustrate the mismatching between regional deformation and faults, we use the "nearneighbor" module built into GMT (The Generic Mapping Tools) to interpolate the Leveling and GPS data to obtain the current regional crustal vertical motion velocity field map (**Figure 6(b)**. Nearneighbor reads arbitrarily located (x, y, z) triples [quadruplets] and uses a nearest neighbor algorithm to assign a weighted average value to each node that has one or more data points within a search radius centered on the node with adequate coverage across a subset of the chosen sectors. The node value is computed as a weighted mean of the nearest point from each sector inside the search radius (https://www.pygmt.org/latest/api/generated/pygmt.nearneighbor.html). Considering the distance between Leveling benchmarks and GPS stations, we set the search radius as 150 km to ensure that each GPS station can search for valid calculation points within this radius.

The interpolated vertical velocity map further confirms our conjecture that there is a strong mismatch between regional deformation and major active faults. Taking into account the inhomogeneity of the Leveling and GPS sites, we cannot guarantee the local accuracy or the deviation due to the interpolation method. However, on the whole, we seem to be able to observe some new phenomena. For example, the Minshan faulted block does not show a significant decline relative to both sides. On the contrary, the Bikou block shows a significant decline relative to its surrounding blocks, especially when it is bounded by the West Qinling on the north side, the Minshan faulted block and the Sichuan basin on the south side (**Figure 6(b)**. In addition, vertical differential motion of the southern segments of the LMSF-LRBF is closer to the more active foreland (**Figure 6(b)**, in line with or corroborate with some existing understandings [4] [24] [30]).

Wang [23] used nine years of three-dimensional deformation data collected in the aftermath of the 2008 Mw7.9 Wenchuan earthquake to propose that the

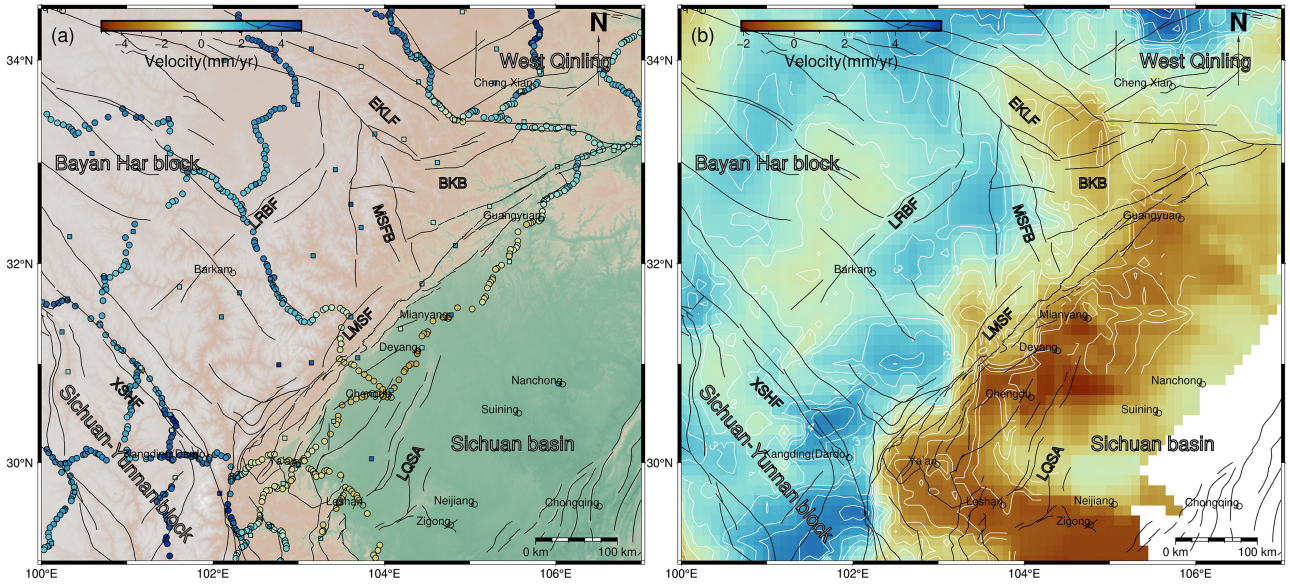

Figure 6. (a) Vertical velocity field relative to ITRF2008 in the study area. Velocities are represented by color-coded circles (Leveling benchmarks) and squares (GPS stations). (b) Interpolated vertical velocity field in the study area. Solid white lines represent contours. Other content is the same as **Figure 1**.

rheological structure of the eastern Tibet lithosphere is consistent with a "jelly sandwich" model, in which a relatively weak lower crust underlain by a stronger upper mantle could explain broadly distributed ductile deformation, interseismic coupling between the lower and upper crust and the continuum deformation partly transmitted up to the surface (**Figure 2**, **Figure 4**, **Figure 6**). This model is equally applicable to explaining the deformation characteristics revealed by the present-day vertical motion field in the region that we observe.

4. Discussion

Taking advantage of the latest GPS data for detecting the deformation in the Longmenshan-Longriba region, the velocity profiles crossing the Longmenshan-Longriba fault zone show that both the LMSF and LRBF have the property of right-lateral strike-slip and thrust movement, although the magnitude of the slip rate varies between segments (**Figure 3**), it is acceptable that the Longmenshan-Longriba fault zone, as block boundary faults, is still the main body for absorbing and adjusting the crustal strain and tectonic deformation. We also noticed that the focal mechanism solutions of the LRBF and the XSHF are dominated by strike-slip, while the LMSF is dominated by thrust. This is consistent with the kinematic mechanism obtained from the GPS velocity field and geological results (**Figure 2**, **Figure 3**, [7] [27]), reflecting the LRBF and LMSF play different roles in regulating crustal movement and upper crustal deformation. The Longmen Shan sub-block is under the combined action of eastward extrusion from the Tibetan Plateau and northwestward push of the Sichuan Basin, resulting in dextral slip along the LRBF and thrust slip with dextral component along the Longmen Shan [7].

The strain rate field (**Figure 4**) based on GPS data in the Longmenshan-Longriba region is calculated to reveal the potential area of high strain rate and high seismic risk. In addition to the elastic strain build-up around LRBF, the strain-rate field is also found to be broadly distributed, suggesting that the deformation field is at least partially coupled with and dictated by a mechanically weakened lower crust [23]. Different from the LRBF, The strain distribution on the LMSF is non-uniform. The strain variation on the LMSF may be controlled by several different dynamic sources, namely: the northern segment plays a role in transferring material to the northeast through the dextral dislocation, causing a lowest strain rate; controlled by the south-eastward pushing of the Bayan Har block, the central segment received the greatest cumulative strain [33], concentrated on the BYF; while the southern segment is controlled by the south-eastward pushing of the Bayan Har block and the eastward pushing of the Sichuan-Yunnan block [24], making the tectonic activity of the southern Longmen Shan move forward.

The strain rate profiles also show different variation characteristics, which may also imply that different segments have different dynamic sources. The magnitude of the strain rate generally shows the phenomenon of increased strain near the fault. The southwestern segment of the LMSF-LRBF near the Xianshuihe fault zone affected by tectonic superposition, has the highest values, while the middle and northeastern segments are comparable. Although this model still needs further geophysical evidence and geodynamic modeling.

What makes us interested is that several large earthquakes in this region since 1970 just correspond to the high-strain areas (**Figure 1**, **Figure 4**), for example, the 2008 Mw7.9 Wenchuan earthquake, the 2013 Mw6.6 Lushan earthquake, the 2022 Mw6.7 Luding earthquake. In addition, the earthquake activity surrounding the Longmenshan-Longriba region appears to have been ongoing. For example, the 2022 Mw5.8 Lushan earthquake nearly occurred at the same location as the 2013 Mw6.6 Lushan earthquake (**Figure 1**, **Figure 4**). Whether this earthquake is an aftershock or a separate earthquake is debatable. The Dayi seismic void located between the 2008 Wenchuan earthquake zone and the 2013 Lushan earthquake zone is a 40 - 60 km long area without earthquakes. The latest borehole in-situ stress measurements confirmed that the vicinity of the Shuangshi-Dachuan fault zone (Dachuan Town) in the Dayi earthquake void is in a state of high in-situ stress, which has the necessary conditions for frictional sliding, and has the potential danger of moderate and strong earthquakes [34] [35]. On June 10, 2022, an earthquake of magnitude Mw5.9 occurred in Malcon City, Sichuan Province (32.25 degrees; 101.82 degrees), with a focal depth of 13 km and an altitude of 3590 m. This earthquake is a typical earthquake cluster event, although its seismogenic structure is still unclear, but it is of great significance for us to understand the tectonic activity and earthquake risk in this area (**Figure 1**, **Figure 4**). The 2020 Ms4.8 Longquanshan earthquake further confirms the tectonic activity of the Longmen Shan foreland. These evidence shows that the strain rate field can provide us a strong scientific basis for tectonic de-

formation monitoring and earthquake risk zone prediction. At the same time, these high-strain areas may still be high-risk areas for earthquakes in the future.

Precise Leveling data combined with GPS data provided us with first-hand information on the present-day vertical crustal motion characteristics in the Longmenshan-Longriba region (**Figure 6**). A mismatch exists between vertical deformation and faults in this region revealed by the Leveling profiles (**Figure 6(a)**. Through valid spatial interpolation, we obtained the regional vertical deformation field (**Figure 6(b)**), exhibiting a decoupling between the regional deformation and active faults, which can only be attributed to the incomplete coupling of deformation between the lower and upper crust. Therefore, we prefer that the eastward extrusion of Tibet is absorbed in the Songpan-Ganzi crust, accommodated through faulting of conjugate strike-slip faults in the upper crust and distributed shear in the lower crust [23]. The weaker lower crust deforms passively in response to E-W compression and absorbs horizontal shortening with broadly distributed ductile shear and vertical thickening of the crust [23].

5. Conclusions

Utilizing the dense GPS data and precise Leveling data to analyze the kinematic characteristics and deformation mode of the Longmenshan-Longriba region, we conclude the followings:

1) The LMSF and LRBF, accompanying with dextral strike-slip and thrust movement, are still the main boundary faults for absorbing and adjusting the crustal strain and tectonic deformation.

2) The strain rate field provides us with an accurate image of high strain areas and high seismic risk, providing us with a scientific basis for understanding tectonic activity and earthquake prediction.

3) Regional vertical velocity field shows a mismatch between deformation and active faults, indicating a decoupling between the lower and upper crust.

Acknowledgements

The authors are grateful for constructive reviews and comments from the reviewers. This work has been supported by the National Natural Science Foundation of China (No. 42202255, U1939201) and the Shaanxi Province Natural Science Basic Research Program (No. 2023-JC-QN-0296) and Science and Technology Fund of the Second Monitoring and Application Center of China Earthquake Administration (No.KJ20220103, KJ20220205).

Conflicts of Interest

The authors declare no conflicts of interest regarding the publication of this paper.

References

[1] Royden, L.H., Burchfiel, B. and van der Hilst, R. (2008) The Geological Evolution of

the Tibetan Plateau. *Science*, **321**, 1054-1058. https://doi.org/10.1126/science.1155371

[2] Hubbard, J. and Shaw, J.H. (2009) Uplift of the Longmen Shan and Tibetan plateau, and the 2008 Wenchuan (M = 7.9) earthquake. *Nature*, **458**, 194-197. https://doi.org/10.1038/nature07837

[3] Wang, M., Jia, D., Shaw, J., Hubbard, J., Plesch, A., Li, Y. and Liu, B., (2014) The 2013 Lushan Earthquake: Implications for Seismic Hazards Posed by the Range Front Blind Thrust in the Sichuan Basin, China. *Geology*, **42**, 915-918. https://doi.org/10.1130/G35809.1

[4] Li, W., Zhang, S.M., Jiang, D.W. and Gao, Y. (2017) Thrust of the Southern Longmenshan Fault Zone in the Late Quaternary Revealed by River Landforms. *Seismology and Geology*, **39**, 1213-1236. (In Chinese)

[5] Guo, X., Gao, R., Keller, G., Xu, X., Wang, H. and Li, W. (2013) Imaging the Crustal Structure Beneath the Eastern Tibetan Plateau and Implications for the Uplift of the Longmen Shan Range. *Earth and Planetary Science Letters*, **379**, 72-80. https://doi.org/10.1016/j.epsl.2013.08.005

[6] Xu, X., Wen, X., Chen, G. and Yu, G. (2008) The Discovery of the Longriba Fault Zone in the East of the Bayan Har Block and Its Tectonic Significance. *Science in China*, **38**, 529-542. (In Chinese)

[7] Ren, J., Xu, X., Yeats, R. and Zhang, S. (2013) Latest Quaternary Paleoseismology and Slip Rates of the Longriba fault Zone, Eastern Tibet: Implications for Fault Behavior and Strain Partitioning. *Tectonics*, **32**, 216-238. https://doi.org/10.1002/tect.20029

[8] Wang, M. and Shen, Z. (2020) Present-Day Crustal Deformation of Continental China Derived from GPS and Its Tectonic Implications. *Journal of Geophysical Research*: *Solid Earth*, **125**, e2019JB018774. https://doi.org/10.1029/2019JB018774

[9] Deng, Q.D., Chen, S.F. and Zhao, X.L. (1994) Tectonics, Scismisity and Dynamics of Longmenshan Mountains and Its Adjacent Regions. *Seismology and Geology*, **16**, 389-403. (In Chinese)

[10] Xu, X., Wen, X., Yu, G., Chen, G., Klinger, Y., Hubbard, J. and Shaw, J. (2009) Coseismic Reverse- and Oblique-Slip Surface Faulting Generated by the 2008 Mw 7.9 Wenchuan Earthquake, China. *Geology*, **37**, 515-518. https://doi.org/10.1130/G25462A.1

[11] Ran, Y.K., Shi, X., Wang, H., Chen, L.C., Chen, J., Liu, R.C. and Gong, H. (2010) The Maximum Coseismic Vertical Surface Displacement and Surface Deformation Pattern Accompanying the Ms 8.0 Wenchuan Earthquake. *Chinese Science Bulletin*, **55**, 841-850. (In Chinese)

[12] Zhang, P.-Z., Shen, Z., Wang, M., Gan, W., Burgman, R., Molnar, P., Wang, Q., Niu, Z., Sun, J., Wu, J., Sun, H. and You, X. (2004) Continuous Deformation of the Tibetan Plateau Constrained from Global Positioning Measurements. *Geology*, **32**, 809-812. https://doi.org/10.1130/G20554.1

[13] Wang, Y.Z., Wang, E.N., Shen, Z.K., Wang, M., Gan, W.J., Qiao, X.J., Meng, G.J., Li, T.M., Tao, W., Yang, Y.L., Chen, J. and Li, P. (2008) Constrained Inversion of Present Activity Rates of Major Faults in Sichuan-Yunnan Region Based on GPS Data. *Science in China*, **38**, 582-597. (In Chinese)

[14] Li, Y., and Zhou, R.J. (2006) Geomorphic Evidence for the Late Cenozoic Strike-Slipping and Thrusting in Longmen Mountain at the Eastern Margin of the Tibetan Plateau. *Quaternary Sciences*, **26**, 40-51. (In Chinese)

[15] Ma, B.Q., Su, G., Hou, Z.H. and Shu, S.B. (2005) Late Quaternary Slip Rate in the

Central Part of the Longmenshan Fault Zone from Terrace Deformation Along the Minjiang River. *Seismology and Geology*, **27**, 234-242. (In Chinese)

[16] Shen, Z.-K., Lü, J., Wang, M. and Bürgmann, R. (2005) Contemporary Crustal Deformation around the Southeast Borderland of the Tibetan Plateau. *Journal of Geophysical Research*: *Solid Earth*, **110**, Article No. B11409. https://doi.org/10.1029/2004JB003421

[17] He, J.J., Ren, J.J., Ding, R., Xu, X.W., Zhao, J.X. and Hu, X.P. (2016) Late Quaternary Activity of the Southern Segment of Longriba Fault Zone in Eastern Tibet and Its Tectonic Implications. *Earthquake Disaster Prevention Technology*, **11**, 707-721. (In Chinese)

[18] Sandwell, D. and Wessel, P. (2016) Interpolation of 2-D Vector Data Using Constraints from Elasticity. *Geophysical Research Letters*, **43**, 10,703-10,709. https://doi.org/10.1002/2016GL070340

[19] Wessel, P., Smith, W., Scharroo, R., Luis, J. and Wobbe, F. (2013) Generic Mapping Tools: Improved Version Released. *Eos*, *Transactions American Geophysical Union*, **94**, 409-410. https://doi.org/10.1002/2013EO450001

[20] Sun, H., He, H., Ikeda, Y., Kano, K., Shi, F., Gao, W., Echigo, T. and Okada, S. (2015) Holocene Paleoearthquake History on the Qingchuan Fault in the Northeastern Segment of the Longmenshan Thrust Zone and Its Implications. *Tectonophysics*, **660**, 92-106. https://doi.org/10.1016/j.tecto.2015.08.022

[21] Tian, J. and Lin, Z. (2021) Late Quaternary Activity of the Qingchuan Fault, Eastern Tibetan Plateau Margin: Insights from Stream Channel Offsets and Catchment Erosion. *Geomorphology*, **395**, Article ID: 107949. https://doi.org/10.1016/j.geomorph.2021.107949

[22] Gan, W., Zhang, P., Shen, Z., Niu, Z., Wang, M., Wan, Y., Zhou, D. and Cheng, J. (2007) Present-Day Crustal Motion within the Tibetan Plateau Inferred from GPS Measurements. *Journal of Geophysical Research*: *Solid Earth*, **112**, Article No. B08416. https://doi.org/10.1029/2005JB004120

[23] Wang, M., Shen, Z., Wang, Y., Bürgmann, R., Wang, F., Zhang, P., Liao, H., Zhang, R., Wang, Q., Jiang, Z., Chen, W., Hao, M., Li, Y., Gu, T., Tao, W., Wang, K. and Xue, L. (2021) Postseismic Deformation of the 2008 Wenchuan Earthquake Illuminates Lithospheric Rheological Structure and Dynamics of Eastern Tibet. *Journal of Geophysical Research*: *Solid Earth*, **126**, e2021JB022399. https://doi.org/10.1029/2021JB022399

[24] Jiang, D.W., Zhang, S.M., Li, W. and Ding, R. (2018) Foreland Deformation Pattern of the Southern Longmen Shan in Late Quaternary. *Chinese Journal of Geophysics*, **61**, 1949-1969. (In Chinese)

[25] Shen, Z., Wang, M., Zeng, Y. and Wang, F. (2015) Optimal Interpolation of Spatially Discretized Geodetic Data. *Bulletin of the Seismological Society of America*, **105**, 2117-2127. https://doi.org/10.1785/0120140247

[26] Wen, X.-Z., Ma, S.-L., Xu, X.-W. and He, Y.-N. (2008) Historical Pattern and Behavior of Earthquake Ruptures along the Eastern Boundary of the Sichuan-Yunnan Faulted-Block, Southwestern China. *Physics of the Earth and Planetary Interiors*, **168**, 16-36. https://doi.org/10.1016/j.pepi.2008.04.013

[27] Wan, Y.K., Shen, X.Q., Liu, R.F., Liu, X., Zheng, Z.J., Li, Y., Zhang, Y. and Wang, L. (2021) Present Slip and Stress Distribution of Block Boundary Faults in the Sichuan-Yunnan Region. *Seismology and Geology*, **43**, 1614-1637. (In Chinese)

[28] Li, K., Xu, X.-W., Tan, X.-B., Chen, G.-H., Xu, C. and Kang, W.-J. (2015) Late Quaternary Deformation of the Longquan Anticline in the Longmenshan Thrust Belt,

Eastern Tibet, and Its Tectonic Implication. *Journal of Asian Earth Sciences*, **112**, 1-10. https://doi.org/10.1016/j.jseaes.2015.08.022

[29] Xu, F., Lu, R.Q., Wang, S., Jiang, G.Y., Long, F., Wang, X.S., Su, P. and Liu, G.S. (2022) Study on the Seismotectonics of the Qingbaijiang M_S5.1 Earthquake in Sichuan Province in 2020 by Multiple Constraint Method. *Seismology and Geology*, **44**, 220-237. (In Chinese)

[30] Tan, X.B., Li, Y.X., Xu, X.W., Chen, M.Y., Xu, C. and Yu, G.H. (2013) Cenozoic Fault Activity of the Southern Segment of the Longmenshan Thrust Belt: Evidence from Low-Temperature Thermochronology Data. *Seismology and Geology*, **35**, 506-517. (In Chinese)

[31] Hao, M., Wang, Q., Shen, Z., Cui, D., Ji, L., Li, Y. and Qin, S. (2014) Present Day Crustal Vertical Movement Inferred from Precise Leveling Data in Eastern Margin of Tibetan Plateau. *Tectonophysics*, **632**, 281-292. https://doi.org/10.1016/j.tecto.2014.06.016

[32] Liang, S., Gan, W., Shen, C., Xiao, G., Liu, J., Chen, W., Ding, X. and Zhou, D. (2013) Three-Dimensional Velocity Field of Present-Day Crustal Motion of the Tibetan Plateau Derived from GPS Measurements. *Journal of Geophysical Research: Solid Earth*, **118**, 5722-5732. https://doi.org/10.1002/2013JB010503

[33] Li, H.B., Xu, Z.Q., Ma, S.L. and Zhao, J.M. (2018) Research Progress on Faulting and Dynamic Processes of the 2008 Wenchuan and 2017 Jiuzhaigou Earthquakes: To Commemorate the 10th Anniversary of the Wenchuan Earthquake. *Chinese Journal of Geophysics*, **61**, 1653-1665. (In Chinese)

[34] Zheng, Y. and Guo, R.M. (2021) Study on the Hazard of the Space between the Wenchuan-Lushan Earthquakes: Current Situation, Thinking and Challenges. *Scientia Sinica* (*Terrae*), **51**, 483-486. (In Chinese)

[35] Li, B., Xie, F., Huang, J., Xu, X., Guo, Q., *et al.* (2022) *In Situ* Stress State and Seismic Hazard in Dayi Seismic Gap of Longmenshan Thrust Belt. *Science China: Earth Sciences*, **65**, 1388-1398. https://doi.org/10.1007/s11430-021-9915-4